Liquid Crystals
Publication details, including instructions for authors and subscription information:
http://www.informaworld.com/smpp/title~content=t713926090

Propagative patterns in the convection of a nematic liquid crystal

A. Joets[a]; R. Ribotta[a]
[a] Laboratoire de Physique des Solides, Bat. 510, Université de Paris-Sud, Orsay, France

To cite this Article Joets, A. and Ribotta, R.(1989) 'Propagative patterns in the convection of a nematic liquid crystal', Liquid Crystals, 5: 2, 717 — 724
To link to this Article: DOI: 10.1080/02678298908045421
URL: http://dx.doi.org/10.1080/02678298908045421

LIQUID CRYSTALS, 1989, VOL. 5, NO. 2, 717–724

Propagative patterns in the convection of a nematic liquid crystal

by A. JOETS and R. RIBOTTA
Laboratoire de Physique des Solides, Bat. 510, Université de Paris-Sud, 91405 Orsay, France.

We show here that the convective instability of a nematic liquid crystal subjected to an A.C. electric field (the conduction regime), is never stationary, contrary to the widely accepted picture. Indeed, we have found that the roll structure translates uniformly along the wavevector direction. In the low frequency part of the conduction regime, the structure is rather homogeneous in space and travels at a very low velocity, while inside the high frequency part, the rolls are localized inside stable domains and the propagation velocity is higher by three orders of magnitude. Closer to the cut-off frequency, we have also found a novel time dependent state, where the amplitude of the rolls oscillates periodically in time.

1. Introduction

It is well known that a layer of nematic liquid crystal with negative dielectric anisotropy, in a planar geometry and subjected to an A.C. electric field bifurcates to a space periodic convective state when the voltage is increased above a well-defined threshold [1, 2]. It was believed until very recently that the convective structure at onset (the so-called Williams domains) is stationary inside the whole conduction regime ($f < f_c$, where f_c is the cut-off frequency) [2]. We show here, using an accurate technique, that inside the whole range of the conduction regime the structure at threshold is in fact travelling with a uniform velocity. There are two apparent regimes: a low frequency range, which has extensively been studied, inside which the structure is rather homogeneous in space and propagates with a low velocity, and a high frequency range, where the rolls propagate with a high velocity inside well localized, stable domains [3]. We also report on another novel effect (observed just below f_c) of an oscillation in time of the amplitude of the localized velocity field; this might be the first observation of a breather in convection.

2. The experimental set-up

The experimental set-up is the classical one for the study of electro-hydro-dynamical (E.H.D.) instabilities in a planar geometry. A layer of nematic liquid crystal (Merck Phase V) of negative dielectric anisotropy ε_a was sandwiched between two glass plates coated with semi-transparent electrodes. The alignment is made homogeneous in the plane of the plates: **n** is parallel to the x axis. An A.C. voltage is applied across the layer, so that the electric field is directed along the z-axis. The applied constraint is measured by the dimensionless parameter $\varepsilon = (V^2 - V_{th}^2)/V_{th}^2$, where V_{th} is the voltage at threshold. The frequency, f, of the excitation is an additional parameter, which is kept fixed for each experiment. The thickness of the sample L_z is typically 50 μm and the lateral dimensions are $L_x = 2{\cdot}5$ cm and $L_y = 1{\cdot}5$ cm, so that the aspect ratio in the wavevector direction is of order 500. The layer can thus be considered as infinitely wide, as compared to the scale of the most unstable modes (the wavelength λ). The sample is enclosed in a container thermally regulated with a water bath; the temperature is kept constant to within at least $\pm 0\cdot1$°C around 21°C for more than five hours.

Because of the coupling between the velocity gradients and the director orientation, any convective flow periodic in space induces a periodic modulation of the optic axis of the crystal. Transmitted light with extraordinary polarization is periodically focused along lines in a horizontal plane parallel to the plates [4]. Small glass spheres (3–5 μm in diameter) are immersed in the layer to trace the streamlines of the convective flow. The focal lines correspond to the vertical (up and down) motion.

The optical pattern in the focal plane was recorded through a CCD 512 × 512 pixel camera and analysed by digital image processing. A line parallel to the x axis was selected at the same height inside the image and its profile is a measure of the transmitted intensity $I(x)$ along this line. Successive images were recorded periodically with a time interval δt (typically $\delta t = 0\cdot3$ s), and the lines were plotted one above the other [5]. The resulting figure is a space-time diagram, where the intensity I is represented as a function of the coordinate x and of the time t (see figure 1).

The convective state develops above a well-defined threshold $V_{th}(f)$. For intermediate frequencies ($f \approx f_c/2$), the structure at onset is periodic in space with parallel rolls, aligned along the y axis (i.e. normal rolls). The intensity profile $I(x)$ is a periodic succession of peaks separated by $\lambda = 2\pi/k$, the period of the convection ($\lambda = 2d$, where d is the roll diameter; k is the wavevector). In the space-time diagram $\{I, t\}$, the intensity peaks are aligned on straight lines the slope of which $dt/dx = u^{-1}$, where u is the translation velocity of the whole pattern along the x-axis. Peak lines parallel to the t-axis would indicate a purely stationary pattern. Such space-time diagrams can be recorded over long times (up to several hours) and are particularly convenient to characterize states which are slowly varying in time. The accuracy of the measurements is limited by the spatial resolution of the individual peaks and by the spatial homogeneity of the structure (absence of moving defects). In our experiments, we have been able to measure velocities u as low as 10 Å/s $\approx 1\cdot5 \times 10^{-5}\,\lambda$/s in uniform motion over 10^4 s.

3. The non-stationarity of the rolls inside the conduction regime

The eventual propagation velocity, u, is measured for different frequencies of the electric field spanning the whole conduction regime up to the cut-off. Figure 1 is a space-time diagram for the classical normal rolls obtained at intermediate frequencies ($f = 300$ Hz) and for a sample thickness of 50 μm. It shows clearly that the rolls propagate and u is found to be about $10^{-4}\,\lambda$/s. At lower frequencies, below a triple (Lifshitz) point f_m ($f_m \approx 120$ Hz), the rolls at threshold are no longer normal to the y axis, but are tilted symmetrically (oblique rolls structure [6]). We find that this pattern travels also, with almost the same velocity. Increasing the frequency up to f_c, we find that u increases sharply above some frequency $f_l \approx 0\cdot6 f_c$ (see figure 2). In this range of high frequencies, u has a typical value of about $0\cdot5\,\lambda$/s. Here, the pattern loses its spatial homogeneity, and the rolls are localized inside small domains. These results clearly show that inside the whole conduction regime, the director distortion is not stationary and that the tilt angle ψ between the director and the x axis is a slow, periodic function of time

$$\psi = \psi_0 \cos(kx - \Omega t)$$

where $\Omega = ku$.

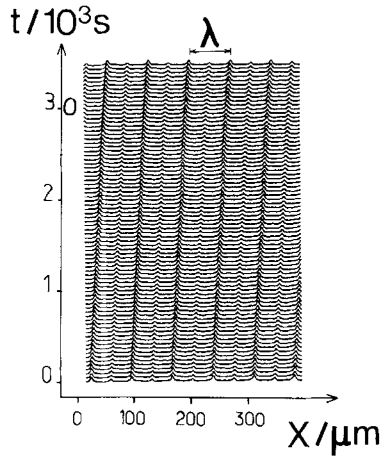

Figure 1. Space-time diagram for the normal rolls ($L_z = 50\,\mu$m, $f = 300$ Hz, $V = 10{\cdot}5$ V, $\varepsilon = 0{\cdot}1$, $\lambda = 70\,\mu$m). The peaks correspond to the upward motion between two rolls. They are aligned along oblique straight lines, from the slope of which the small constant propagation velocity $u = 6{\cdot}5 \times 10^{-3}\,\mu$m/s $= 0{\cdot}9 \times 10^{-4}\,\lambda$/s can be measured.

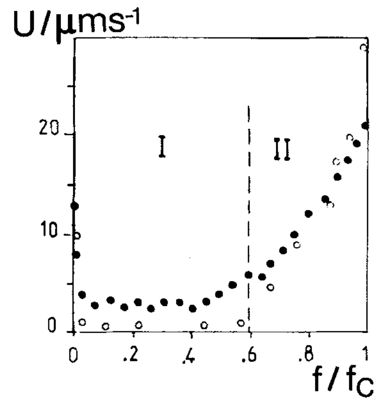

Figure 2. Propagation velocity u at threshold versus the frequency f (●, $L_z = 5\,\mu$m; ○, $L_z = 10\,\mu$m). The conduction regime is divided into two parts. I, the low frequency range where the structure is quasi-homogeneous and travels at low velocity; II, the high frequency range, where the structure is localized in space and travels with a higher velocity. For these values of L_z ($L_z < 20\,\mu$m), the velocity u increases with decreasing frequencies close to D.C.

We have measured the propagation velocity u for different samples of thickness ranging from 5 to 250 μm. In this range the pattern of rolls is always found to travel with a finite drift velocity, in apparent contradiction to the behaviour reported in [7]. The velocity at a given reduced frequency f/f_c increases as the thickness decreases. Moreover, for small thicknesses $L_z < 20\,\mu$m and low frequencies, it is also found that u increases up to $0{\cdot}5\,\lambda$/s for frequencies decreasing to D.C. (see figure 2). Simultaneously, the convective structure is here too, not fully homogeneous in space, but propagates inside domains of large lateral extension (the typical dimensions l_x and l_y of the domains are of order 50–100 d).

4. The localized travelling roll structure

The frequency is fixed at some value inside the high frequency part of the conduction regime: $f \approx 0{\cdot}8 f_c = 600$ Hz (here $f_c \approx 750$ Hz). The voltage is increased smoothly from zero up to a threshold, V_{th}, of 15 V. The pattern at threshold appears inhomogeneous in space and consists of isolated domains of elliptical-like shape, inside which a periodic structure of rolls aligned along y translates uniformly in the x direction (see figure 3). The typical value of the propagation velocity u is about 10 μm/s. Very close to the threshold ($\varepsilon = 0{\cdot}1$), the lateral dimensions of a domain are typically $l_x = 3d$ and $l_y = 4d$. These domains are randomly spread in the plane of the layer, and no deformation of the director alignment is detected in the space between them. They remain stable in space, thus indicating a nearly zero group velocity. In this travelling wave structure, the convective variables behave like $A(x)\cos(kx - \Omega t)$. It is found that, for a typical domain, the amplitude $A(x)$ has a lump shape which can be fitted fairly well to a $\mathrm{sech}^2(x/l_x)$ function, which is typical of a soliton-like profile [3]. Space–time diagrams are plotted for increasing values of the voltage and u is found to be finite at threshold, while the amplitude of the instability measured by the transmitted light intensity increases continuously from zero. Simultaneously, the domains increase their extension in both directions, so that they get closer to each other and connect completely as the constraint parameter, ε, tends to 1. These connection boundaries reveal new and particularly interesting problems. They correspond to topological defects of the non-linear travelling waves [8] which represent the propagating rolls. When a connecting boundary between two domains of opposite velocity is along the rolls axis, either a source or a sink state is obtained when the waves leave or meet at the boundary, respectively. Sources or sinks may also occur spontaneously inside a single domain. For $\varepsilon > 1$, the velocity u falls rapidly to zero and a quasistationary, homogeneous state is recovered. The velocity measured at threshold decreases sharply and continuously as the frequency is decreased down to some value f_l (here $f_l = 530$ Hz), where the slow propagation regime of intermediate frequencies is met. Then the velocity falls by two orders of magnitude over a range $\Delta f \approx 10$–20 Hz. Simultaneously, the size of the domains diverges and the normal rolls

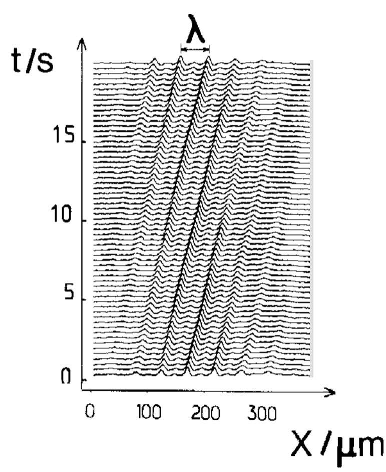

Figure 3. Space time diagram for the localized travelling structure. The rolls are travelling to the right with a velocity $u = 5{\cdot}8\ \mu$m/s. ($L_z = 50\ \mu$m, $f = 600$ Hz, $V = 15{\cdot}9$ V, $\varepsilon = 0{\cdot}3$). The domain contains five wavelengths λ.

are recovered. The propagation of the pattern means that the director field is propagating along the x axis. The velocity field $\mathbf{v}$ is then expected to propagate in the same way. However, this does not imply that the fluid particles have an average velocity equal to u. The real flow structure can be characterized from the space-time representation by tracing the trajectories of individual particles immersed in the nematic material. The experimental procedure consists in recording the profile of a line which includes a particle at every time. Provided that the ratio v_y/v_x inside a roll is small, a particle can easily be automatically followed by the digital processor. The lagrangian trajectory in the x–t space is obtained therefore. Two types of trajectories are found inside the propagating structure [5]. In the first one, which we call the closed flow, the particles have an average velocity $\bar{v}_x$ equal to u. Their motion is composed of a rotation around the rolls axis and a uniform translation with velocity u. The closed flow is an ensemble of closed cells propagating with velocity u. In the second type of trajectories, the open flow, the particles translate mainly in the opposite direction to that of the travelling wave, along an open curve, between the closed cells. The total flow is then decomposed into two components. Figure 4 shows a sketch of the flow structure in the comoving frame of the travelling rolls. The precise topology of this complex time-dependent velocity field can be well described using a simple kinematic model [9]. Between the rolls domains, where the director alignment is not distorted, the particles have a very small constant velocity ($\approx 0{\cdot}5\,\mu$m/s) in the plane of the layer. More recently, from experimental observations of global mass transport in propagative convection of a binary mixture, other authors have deduced similar flow structures and compared them to an identical model [10]. We believe that only the knowledge of the individual trajectories can correctly verify this model.

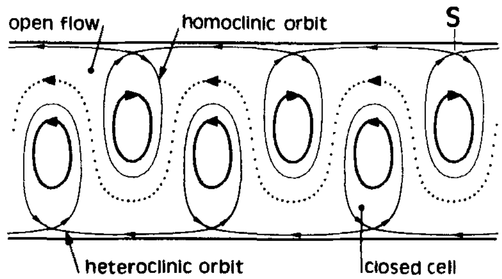

Figure 4. Representation of the flow structure in the comoving frame of travelling rolls ($v_x = -\partial\zeta/\partial z, v_z = \partial\zeta/\partial x$, where $\zeta = \zeta_0 \sin(kx - \Omega t)$). The closed flow is bounded by homoclinic orbits connected by heteroclinic ones at the stagnation points S.

The one dimensional theoretical model [11] which was developed soon after the discovery of these E.H.D. instabilities, as well as the two or three dimensional extensions [12] are unable to account for travelling rolls. We now give some observations which should be taken into account to improve the model. At high frequencies, the characteristic times τ and τ_c [13] associated, respectively, to the relaxation of the charges and of the director orientation are comparable. (Here $\tau \approx 4 \times 10^{-3}$ s, $\tau_c \approx 25 \times 10^{-3}$ s, for $f = 600$ Hz and $L_z = 50\,\mu$m). The curvature is then less efficient in stabilizing the spatial charge modulation against any possible lateral drift. Indeed, for a slight lateral drift of the charge distribution and within each half-period of the electric field, the curvature will adapt immediately to the new distribution, and the overall pattern can move uniformly as a progressive wave, in the direction of the director, along with a charge-density wave. In the model, such an effect might be included by allowing a D.C. large scale component of the density current to be superimposed onto the actual space-periodic distribution. Secondly, the initial model assumes that the time-dependence of the force can be averaged out. Such an assumption, which implies that the curvature is stationary in time, is less valid near the cut-off frequency. We may then suggest that, when the relaxation time for the curvature becomes comparable to the period of the electric field, the coupling between the curvature and the large scale drift motion of the charges is more efficient. Obviously this occurs close to D.C., but also close to the cut-off where the large value of the voltage reduces the curvature time to values close to the period. The decrease of the drift velocity at intermediate frequencies would be due to the pinning effect by a more efficient focusing of the charges at the rate of the driving field. The thickness dependence of the drift velocity may be ascribed to the E-field dependent drift by a Coulomb force, while the instability threshold is a voltage threshold. Hence the drift is larger for thinner samples.

The spatial inhomogeneity cannot be understood at the present time with the results at hand, especially at low frequencies. The same experiments were also performed with Mylar sheets ($5\,\mu$m) thick, covering the electrodes and led to similar observations. Charge injection by the plate is probably unimportant. A purely phenomenological mechanism can be suggested for the strong localization effect observed at high frequencies, which is based on an analogy of these travelling rolls with non-linear surface waves (i.e. Stokes waves) [14]. It is possible that in the range of frequencies where localization takes place, the dispersive effects in the phase dynamics, as well as the non-linearities, become important even very close to the onset. Then, when the voltage reaches the threshold, the fastest disturbance which grows out of the rest state is not defined by a unique wavevector k, but rather by a broad band Δk centred on a value close to the critical one k_c. In real space, this corresponds to a space modulation of the amplitude of the convective state. Such a modulational instability can develop under some conditions (i.e. the Benjamin–Feir criterion [15]), and the tendency to localization may be reinforced by the non-linearities (i.e. self-focusing). This type of solution, although not yet fully demonstrated, could arise, as was first suggested by Newell [16, 17], from a complex Landau-Ginzburg equation. This equation, which is known to govern a large class of pattern forming systems, is:

$$\frac{\partial A}{\partial t} = \alpha A + \gamma \frac{\partial^2 A}{\partial x^2} - \beta |A|^2 A,$$

where A is the complex envelope of the rolls and

$$v = \mathrm{Re}(\varepsilon A \exp[i(kx - \Omega t)]$$

The real coefficient α is the linear growth rate of the unstable mode. The two other coefficients are complex. The real part of γ is a measure of the growth rate of sideband modes relatively to α; its imaginary part measures the wave dispersion. The real part of β measures the saturation of the unstable mode and its imaginary part couples the wave frequency to the amplitude A.

4. The breather-like structure

For frequencies f closer to the cut-off frequency f_c ($f \approx 0{\cdot}9 f_c$), a new time dependence may appear at threshold, under conditions which are yet not well defined.

The amplitude of the localized propagative structure is now oscillating simultaneously in time. The convective variables behave as $B(t)A(x)\sin(kx - \Omega t)$, where the amplitude $B(t)$ is a periodic function of time as in the case of breathers [18]. The breathing period T is found to be typically of order 10 s. This state is more easily observed as a transient when a small step of voltage is applied just above threshold. In that case, the breathing amplitude can reach the zero value periodically. The space-time diagram corresponding to the breather-like state is shown on figure 5. Usually, it is found that the domains breath in phase over large areas which include up to ten domains. The origin of this new time-dependent state is not yet understood, although it might be compared to the localized time dependent state studied by Bretherton and Spiegel in the case of thermohaline convection [19]. Note, however, that in their model the domains are uncorrelated in time.

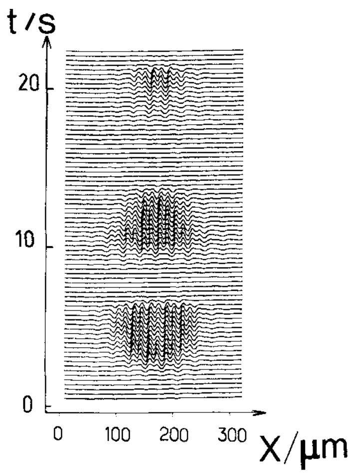

Figure 5. Space-time diagram for the breather-like structure ($L_z = 50\,\mu$m, $f = 700$ Hz, $V = 25$ V, $\varepsilon = 0{\cdot}1$). The envelope of the rolls passes periodically through zero.

5. Conclusion

We have demonstrated experimentally using an accurate technique that, inside the conduction regime, the rest state bifurcates to convective states which are time dependent, contrary to the widely accepted picture. In addition to propagating, these states are heterogeneous in space, except in the range of intermediate frequencies. Another new time dependent state has also been observed in the form of an oscillation in time of the amplitude. These results indicate that electroconvection in a nematic layer is more complex than previously believed (and even experimentally found). We suggest that the essential features of these effects can be described, as in the case of surface waves on shallow water, by the evolution of the amplitude of non-linear waves that in fact could be derived from a typical model such as a complex time-dependent Landau-Ginzburg equation.

References

[1] Williams, R., 1963, *J. chem. Phys.*, **39**, 384.
[2] Orsay Liquid Crystal Group 1970, *Phys. Rev. Lett.*, **25**, 1642.
[3] Joets, A., and Ribotta, R., 1988, *Phys. Rev. Lett.*, **60**, 2164.

[4] De gennes, P.-G., 1974, *The Physics of Liquid Crystals* (Clarendon Press).
[5] Joets, A., and Ribotta, R., 1988, *Propagation in Systems Far from Equilibrium*, edited by J. E. Wesfreid, H. R. Brand, P. Manneville, G. Albinet and N. Boccara (Springer Series in Synergetics, Vol. 40) p. 176.
[6] Ribotta, R., Joets, A., and Lin Lei, 1986, *Phys. Rev. Lett.*, **56**, 1595.
[7] Rehberg, I., Steinberg, V., Zimmermann, W., and Kramer, L., 1988, *Twelfth International Liquid Crystal Conference*, Freiburg, August.
[8] Coullet, P., Elphick, C., Gil, L., and Lega, J., 1987, *Phys. Rev. Lett.*, **59**, 884.
[9] Joets, A., and Ribotta, R. (to be published). A similar model has been proposed independently by Linz, S. J., Lücke, M., Müller, H. W., and Niederländer, J., 1988, *Phys. Rev.* A, **38**, 5727.
[10] Moses, E., and Steinberg, V., 1988, *Phys. Rev. Lett.*, **60**, 2030.
[11] Helfrich, W., 1969, *J. chem. Phys.*, **51**, 4092. Dubois-Violette, E., de Gennes, P.-G., and Parodi, O., 1971, *J. Phys., Paris*, **32**, 305.
[12] Goosens, W. J. A., 1978, *Advances in Liquid Crystals*, Vol. 3, edited by G. H. Brown (Academic Press) p. 1. Bodenschatz, E., Zimmermann, W., and Kramer, L., 1988, *J. Phys., Paris*, **49**, 1875.
[13] The times are defined as $\tau = \varepsilon_{\|}/4\pi\sigma_{\|}$, where $\varepsilon_{\|}$ and $\sigma_{\|}$ are the components of the dielectric constant and the conductivity along the director; $\tau_c^{-1} = \eta^{-1}[(-\varepsilon_a\varepsilon_{\perp}/4\pi\varepsilon_{\|})E^2 + K_{33}k^2]$, where E is the electric field, K_{33} the elastic constant for bend, k the wavevector, ε_a and $\varepsilon_{\perp}$ are respectively the dielectric anisotropy and the dielectric component normal to the director, and η is a bend viscosity.
[14] Benjamin, T. B., and Feir, J. E., 1967, *J. Fluid Mech.*, **27**, 417.
[15] Stuart, J. T., and DiPrima, R. C., 1978, *Proc. R. Soc.* A, **362**, 27.
[16] Newell, A. C., 1979, *Pattern Formation and Pattern Recognition*, edited by H. Haken (Springer) p. 244.
[17] Newell, A. C., 1978, *Solitons in Condensed Matter Physics*, edited by A. R. Bishop and T. Schneider (Springer Series in Solid State Science, Vol. 8) p. 52.
[18] MacLaughlin, D. W., and Scott, A. C., 1978, *Phys. Rev.* A, **18**, 1652.
[19] Bretherton, C. S., and Spiegel, E. A., 1983, *Physics Lett.* A, **96**, 152.